*fibers*

MDPI

*Communication*

# Tolnaftate-Loaded PolyacrylateElectrospun Nanofibers for an Impressive Regimen on Dermatophytosis

**Shashi Kiran Misra [1], Himanshu Pandey [1,2,*], Sandip Patil [3], Pramod W. Ramteke [1] and Avinash C. Pandey [2]**

1 Department of Pharmaceutical Sciences, Sam Higginbottom University of Agriculture, Technology & Sciences, Allahabad 211007, India; shashisarthak@gmail.com (S.K.M.); pwramteke@gmail.com (P.W.R.)
2 Nanotechnology Application Centre, Institute of Interdisciplinary Studies, University of Allahabad, Allahabad 211002, India; dr.avinashcpandey@gmail.com
3 E-Spin Nanotech Pvt. Ltd. SIDBI Centre, Indian Institute of Technology, Kanpur 208016, India; Patilsandip13@gmail.com
* Correspondence: himanshu.nac@gmail.com; Tel.: +91-945-223-5001

Academic Editor: Anil N. Netravali
Received: 10 July 2017; Accepted: 31 October 2017; Published: 6 November 2017

**Abstract:** Dermatophytosis, topical fungal infection is the most common cause of skin bug in the world, generally underestimated and ignored. It is commonly caused by immensely mortifying and keratinophilic fungal eukaryotes which invade keratinized tissues and generate different tinea diseases in Mediterranean countries. We herein fabricated nanofibers/scaffolds embedded with thiocarbamate derivative topical antifungal tolnaftatefor the first time to target the complete elimination of dermatophyte at the site of infection. In this regard, variable combinations of biocompatible Eudragit grades (ERL100 and ERS100) were selected to provide better adhesion on the site of dermatophytosis, ample absorption of exudates during treatment, and customized controlled drug release. Surface topography analysis indicated that the fabricated nanofibers were regular and defect-free, comprising distinct pockets with nanoscaled diameters. Characterization and compatibility studies of tolnaftate, polymers, and their nanofibers were performed through ATR-FTIR, TGA, and PXRD. Remarkable hydrophilicity and an excellent swelling index were obtained from a 3:1 ratio of ERL100/ERS100 electrospun D3 nanofibers, which is an essential benchmark for the fabrication of nanofibrous scaffolds for alleviating dermatophytosis. In vitro drug release investigation revealed that a nonwoven nanomesh of nanofibers could control the rate of drug release for 8 h. A microdilution assay exhibited inhibition of more than 95% viable cells of *Trichophyton rubrum* for 96 h. However, *Microsporum* species rigidly restricted the effect of bioactive antifungal nanofibers and hence showed resistance. In vivo activity on *Trichophyton rubrum* infected Swiss albino mice revealed complete inhibition of fungal pathogens on successive applications of D3 nanofibers for 7 days. This investigation suggests potential uses of tolnaftate loaded polyacrylate nanofibers as dressing materials/scaffolds for effective management of dermatophytosis.

**Keywords:** dermatophytosis; polyacrylate nanofibers; tolnaftate; dressing materials

## 1. Introduction

Dermatophytosis, positioned as the fourth most common disease in the last decade, has affected more than 25% of the world's population. The epidemiology of dermatophytosis is highly influenced by socioeconomic factors, modern lifestyles, immigration from endemic countries, and of course disease states, often caused by filamentous dermatophytes (ringworm). Mostly the anthropophilic *Trichophyton*

and the zoophilic *Microsporum* are graded as disastrous pathogens thatinvade keratinized tissue (skin, nail, scalp, etc.) and generate different tinea diseases in Mediterranean countries. These infections are primarily confined to the outer layers of skin, hair, and nails, where keratin is the dominant structural protein, leading to a wide variety of disease states in the scalp (tinea capitis), feet (tinea pedis), and groin (tinea cruris) and in other body surfaces such as tinea corporis [1].These opportunistic fungal infections chiefly occur in the dead regions of keratinized cells of the stratum corneum and are ubiquitous in the world. Most are benign but can become life threatening in immune-compromised or malnourished populations [2]. Non-specificity, adverse effects, poor efficiency, and a growing resistance of these dermatophytes for traditional drug delivery systems has inspired vast interest from researchers in designing innovative topical antifungal substances with the potential to solve the above problems. Traditional topical therapeutics has poor efficiency in targeting and inhibiting the fungal cells, which are metabolically similar to mammalian cells. Moreover, toxic results have been reported when these therapies are prescribed for prolonged use [3].

In 1963, Noguchi and colleagues reported a series of naphthiomates called tolnaftate, which has topical antifungal activity and acts by selectively inhibiting squalene epoxidase, resulting in accumulated squalene and a deficiency in ergosterol in the cell walls of the fungi [4,5]. It is a lipophilic drug (partition coefficient log P > 5) with a large molecular weight of 307.41 g/mol and a poor aqueous solubility of <0.1 g/100 mL and is expected to show poor transport across the skin [6,7]. Recently, much research has been focused on fabricating three-dimensional nano fibers for applications in tissue engineering, catalysis, biosensors, skin regeneration, and wound healing by virtue of their extensive surface-to-volume ratio, peculiar morphology, sufficient mechanical strength, and plentiful porosity [8,9]. It is emphasized that the high surface area of nanofibers expedite proper gaseous exchange, charter fluid accumulation, or retention, of wound fluid, maintain moisture balance, and preserve aseptic conditions [10], which are eminently fascinating properties in the mitigation of infectious wound healing. Inherent nano scaled interconnected voids/pores within these nano fibers also restrict further penetration of pathogen at the application site, and provide desirable cell interactions to make them competent for designing regenerative medicine [11,12]. Additionally, the incorporation of bioactive agents during the fabrication of nano fibers cater specific and efficient exercising for healing wounds, skin regeneration, gene/DNA delivery, and tissue repairing [13].

Biocompatible cationic poly methacrylates Eudragit RL100 and Eudragit RS 100 (ERL100 and ERS100) are robust and reliable polymers with strong properties for scheming novel topical drug delivery systems owing to their specification for film forming and their adhesion to the target site [14,15]. In this paper, for the first time, a mixture of both polymers is utilized for fabrication of nano fibers through an electro spinning technique aimed at the customization of their permeability and controlled drug release to mitigate dermatophytosis. The process of electro spinning is cost-effective and offers fabrication of numerous polymeric (biodegradable and biocompatible) nanofibrous scaffolds for regenerative medicine [13]. The objectives of this research were to zestfully fabricate tolnaftate-loaded variable blends of ERL100/ERS100, their optimization for the formation of defect-free nanofibers having the virtue of a nano range, a nonwoven mesh, ample absorption capacity, and efficiency for the elimination of dermatophytes at the infected site through controlled drug release. Plasticizer PEG 400 was added to prevent inter-particular aggregation of the tolnaftate in the polymeric mixture. Moreover, it would also provide sufficient flexibility and mechanical strength of the fibers. It has been reported that PEG 400 also acts as a surface modifier and maintains the zeta potential of dispersion for optimum stability [16].

## 2. Materials and Methods

Tolnaftate was received from Belco Pharma, Haryana, India. Biocompatible Eudragit RL100 (ERL100) and Eudragit RS 100 (ERS100) polymers with molecular weight of 150,000 Da were procured as gift samples from Evonik (Rohm Pharma, Darmstadt, Germany). Dermatophyte strains i.e., *M. fulvum* (MTCC 2839), *M. canis* (2820), *T. rubrum* (MTCC 7859), and *M. gypseum* (2855) were procured

from Microbial Type Culture Collection (MTCC), Chandigarh, India. Poly ethylene glycol (PEG 400), RPMI 1640 (Roswell Park Memorial Institute Medium), and MOPS (morpholinepropane sulfonicacid) were purchased from Sigma-Aldrich Chemicals Pvt. Ltd., New Delhi, India. Methanol (MeOH), *N*,*N* dimethylacetamide (DMAc), and dimethyl sulfoxide (DMSO) were of analytical grade and procured from Merck, India.

### 2.1. Fabrication of Tolnaftate-Loaded Polyacrylate Polymeric Nanofibers

Initially 20% w/v ERL100/ERS100 polymers of different ratio (1:3, 1:1, and 3:1) was mixed in a 3:2 composition of solvents methanol and *N*,*N* dimethylacetamide to produce a homogeneous solution. Tolnaftate, 1% w/v, was added into each formed polymeric solution and magnetically stirred at room temperature. Thereafter, the non-aggregated drug-loaded polymeric dispersion was placed into a 10 mL plastic syringe with a 15 mm diameter and a sharp needle, and subjected to electro-spinning (E-Spin, Nanotech IIT, Kanpur, India). A flow rate of 5 µL/min, a 15 kV positive power supply, and a 12 cm distance to the brass collector was set for the electro-spinning process (Figure 1). Ambient parameters temperature and humidity were kept at 28 °C–30 °C and 60–65%, respectively. On application of voltage, generation of electrical force led to the formation of Taylor Cone pendent at needle tip; that was retained on brass collector in form of nanofibers within fraction of seconds [17–19]. The fabricated nanofibers were kept in desiccators for further studies.

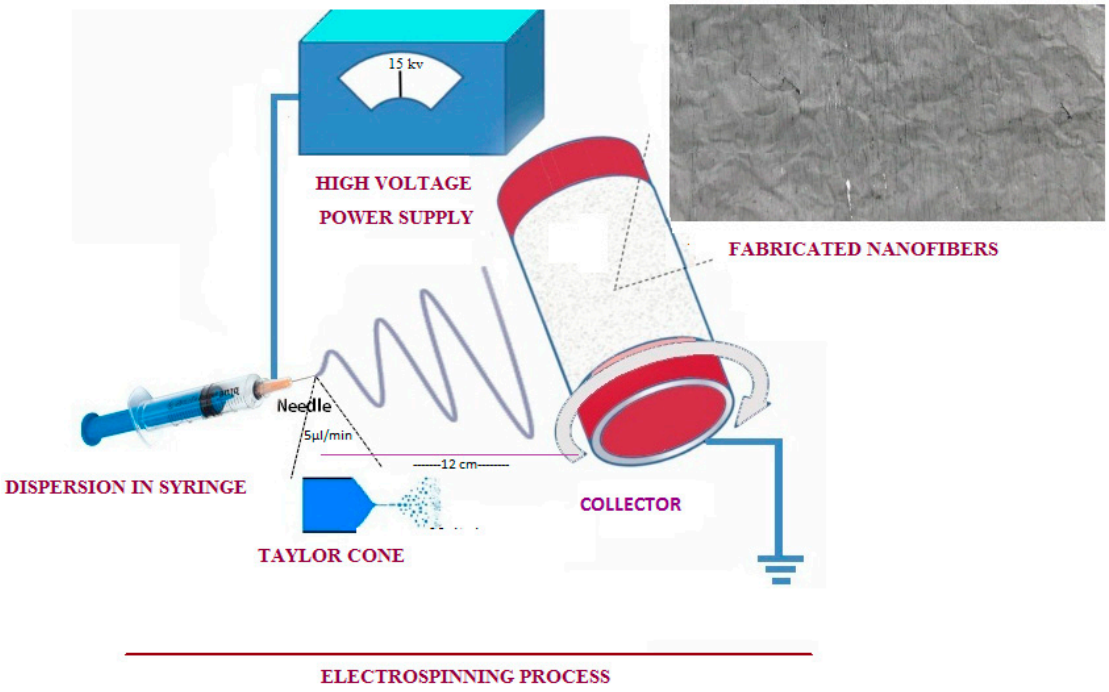


**Figure 1.** Schematic illustration of the process of electro-spinning utilized for the fabrication of nanofibers.

### 2.2. Surface Morphology

Field emission scanning electron microscopy (FESEM quanta 200, Zeiss, Oberkochen, Germany) was utilized to study the surface morphology of the fabricated nanofibers. Prior to the examination, the samples were gold-sputter-coated (approximately 20 nm) under argon to render them electrically conductive. Gold-coated nanofibers were placed in the microscope chamber to which a high vacuum was applied, and the images were taken at an excitation voltage of 15 KV. The average mean diameter and standard deviations were determined from 50 random fibers from three FESEM images. The inset of FESEM images demonstrated the hydrophilic/hydrophobic characteristics of the fabricated

nanofibers, which must influence the initial adhesion on the infected skin and their proliferation to a higher extent [20]. For the determination of hydrophilicity, the static Water contact angle WCAs of nanofibers were measured on a 5 $cm^2$ nanofibrous scaffold through a sessile drop method using a contact angle goniometer (Rame Hart Inc., Succasunna, NJ, USA) equipped with video capture at room temperature. An amount of 30 µL of deionized water was dropped onto five different dried electrospun nanofibers with a micro syringe in an atmosphere of saturated water vapor, and their average values and standard deviations were estimated.

### *2.3. Characterization*

An attenuated total reflectance Fourier transform infrared spectrometer (ATR-FTIR Brukeroptick Gmbh, Ettlingen, Germany) consisting of a DLaTGS detector (Leonardo MW Ltd., Southampton, Hampshire, The United Kingdom) with a geramanium internal reflection element (IRE) crystal was utilized within arange of 3500 $cm^{-1}$–500 $cm^{-1}$ to identify functional groups present in the mixture of polymers, tolnaftate, and their nanofibers. Thermogravimetric analysis (TGA) was performed with a Perkin Elmer TGA-DTA (Diamond series) at a heating rate of 50 °C–600 °C, and the mass changes, as well as the amount of residual material, after heating were analyzed. Identification of the crystalline and amorphous nature of the drug and polymers via X-ray diffraction analysis (X' Pert PRO, PAN analytical, Almelo, The Netherlands) was performed using Cu Kα radiation at the 2θ range of 10°–60° at 40 mV and 300 mA.

### *2.4. Swelling Index and In Vitro Drug Release*

Swelling index of nanofibers is considered an important tool for the estimation of drug release behavior from them. Swelling behavior of fiber mats were carried out in a phosphate buffer with a pH of 6.8 via the gravimetric method [21–23]. The percentage swelling index was calculated by determining the ratio of the weight of water adhered on the nanofibers to the weight of dried nanofibers. For the determination of drug release, dialysis was performed using a dialysis membrane with a pore size of 2.4 nm. Exactly 1 mg of tolnaftate equivalent to the individual nanofibers were kept in 200 mL of the release medium (phosphate buffer pH: 6.8) and stirred at 100 rpm to prevent the formation of a stagnant layer at the bulk and outer solution interface. The aliquots were withdrawn from each medium after every 30 minutes and replaced with the same fresh dissolution medium, maintaining the sink condition. Drug released through nanofibers in the withdrawn aliquots was quantified via UV-spectrophotometer at a $\lambda_{max}$ of 258 nm. The drug release assay was performed in triplicate, and average values were obtained using a straight line equation.

### *2.5. In Vitro Antifungal Assay*

The broth microdilution assay for topical antifungal activity of electrospun D3 nanofibers was performed on four virulent dermatophytes in accordance with the Clinical and Laboratory Standards Institute guidelines (CLSI) for 96 h [22]. In vitro antifungal activity or % growth inhibition was determined on standard Microbial Type Culture Collection (MTCC) strains: *M. fulvum* (MTCC 2839), *M. canis* (MTCC 2820), *T. rubrum* (MTCC 7859), and *M. gypseum* (MTCC 2855) by the CLSI broth microdilution method. Overnight, cultivated different fungal strains were suspended in RPMI-1640 (Sigma Chemical Co, St. Louis, MO, USA) supplemented with L-glutamine and 2% glucose buffered to pH 7 with 0.165 mol/L morpholinepropane sulfonic acid (MOPS) to yield $1 \times 10^5$ CFU/mL in a flat bottomed 96-well microtiter plate [24].

### *2.6. In Vivo Animal Study*

For in vivo study, the experimental protocol was approved by the animal ethical committee, Government of India (BU/Pharm/IAEC/15/01), and four week old male Swiss albino mice (average weight: 20 g–25 g) were used for treatment of dermatophytosis. The dorsal surface of each mouse were disinfected with ethanol (70%) and depilated with normal hair removal cream one day prior to infection.

The conidial suspension of dermatophyte *T. rubrum* was prepared as previously reported [25,26] and inoculated on the dorsal surface of mice and left them for growth of infection. In vivo efficiency of tolnaftate and tolnaftate loaded D3 nanofibers were compared after continuous application treatment for seven days.

## 3. Results and Discussion

### *3.1. Fabrication of Tolnaftate-Loaded Polyacrylatenanofibers*

Drug loaded polyacrylate nanofibers D1, D2, and D3 were successfully fabricated via the electrospinning technique (E-Spin, Nanotech, IIT, Kanpur, India) under preset controlled process parameters, i.e., flow rate, applied voltage, and distance from the syringe tip to the collector.

#### 3.1.1. Surface Morphology

All nanofibers, D1, D2, and D3, were found to be regular and non-beaded, with nonwoven morphology. The average diameters of D1, D2, and D3 nanofibers were estimated through Image J software and reported 462.7 nm ± 40.5 nm, 302.6 nm ± 50.43 nm, and 402.3 nm ± 65 nm, respectively. D2 nanofibers showed that a smaller diameter must be attributed to an equal concentration of both polymers and possessed a uniform network, which is a desirable benchmark for wound healing.

An increased diameter of D1 nanofibers implied the presence of a high concentration of ERS100, which prevents the complete evaporation of the solvents from their surface due to their high relative viscosity. D1, D2, and D3 nanofibers showed average contact angles of 62.1°± 8.9°, 40° ± 6.3°, and 51.5° ± 7.5° respectively, as represented in Figure 2.

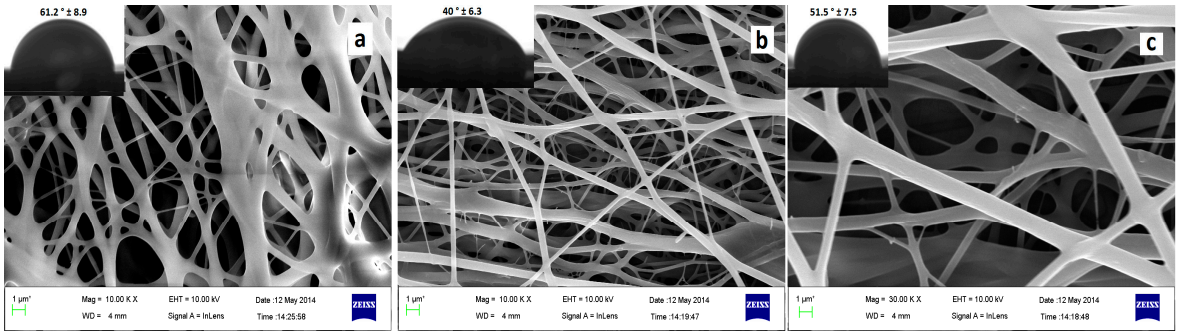


**Figure 2.** FESEM images illustrated surface topography of fabricated D1 nanofibers composed of ERL100/ERS100:1:3 (**a**); D2 nanofibers of ERL100/ERS100: 1:1 (**b**) and D3 nanofibers prepared from ERL100/ERS100: 3:1 (**c**).

A comparatively low contact angle of the D2 nanofibers demonstrated its higher hydrophilicity, attributed to its nanoscaled morphology, which offersan enormous surface area for wetting the nanofiber surface. It was also demonstrated that the hydrophilic behavior of the nanofibrous scaffold were influenced by the diameter of the nanofibers.

#### 3.1.2. Characterizations

Vibrational analysis of tolnaftate suggested C=C stretching mode at 1680 $cm^{-1}$ in the phenyl and naphthalene ring, (responsible for its bioactivity as a fungicide). The asymmetric C-H stretching mode is expected at around 3095 $cm^{-1}$, and the symmetric stretching is expected at 2875 $cm^{-1}$.The C-N-C stretching vibration was observed as a very strong band at 1500 $cm^{-1}$. Tolnaftate consists of a meta disubstituted phenyl ring at 1260 $cm^{-1}$ and the C=S stretching mode was being expected at 1205 $cm^{-1}$ (Figure 3). Moreover, the C-N-C peak in tolnaftate appeared at 1470 $cm^{-1}$, the C=S stretching peak appeared at 1964 $cm^{-1}$, and C-H stretching appeared at 2927 $cm^{-1}$. The presence of the quaternary

ammonium group of both polymers (ERL100/ERS100) was shown by a prominent peak at 3050 $cm^{-1}$ in the IR spectra of tolnaftate-loaded nanofibers and the combination of ERL100/ERS100 polymers. A –COO– peak in the spectra of the blend of two polymers was found at 1728 $cm^{-1}$, and C-H stretching was found at 2926 $cm^{-1}$. Additionally, strong peaks at 1280 $cm^{-1}$ and 1090 $cm^{-1}$ confirmed the O-H and C-O-H stretching of PEG 400.

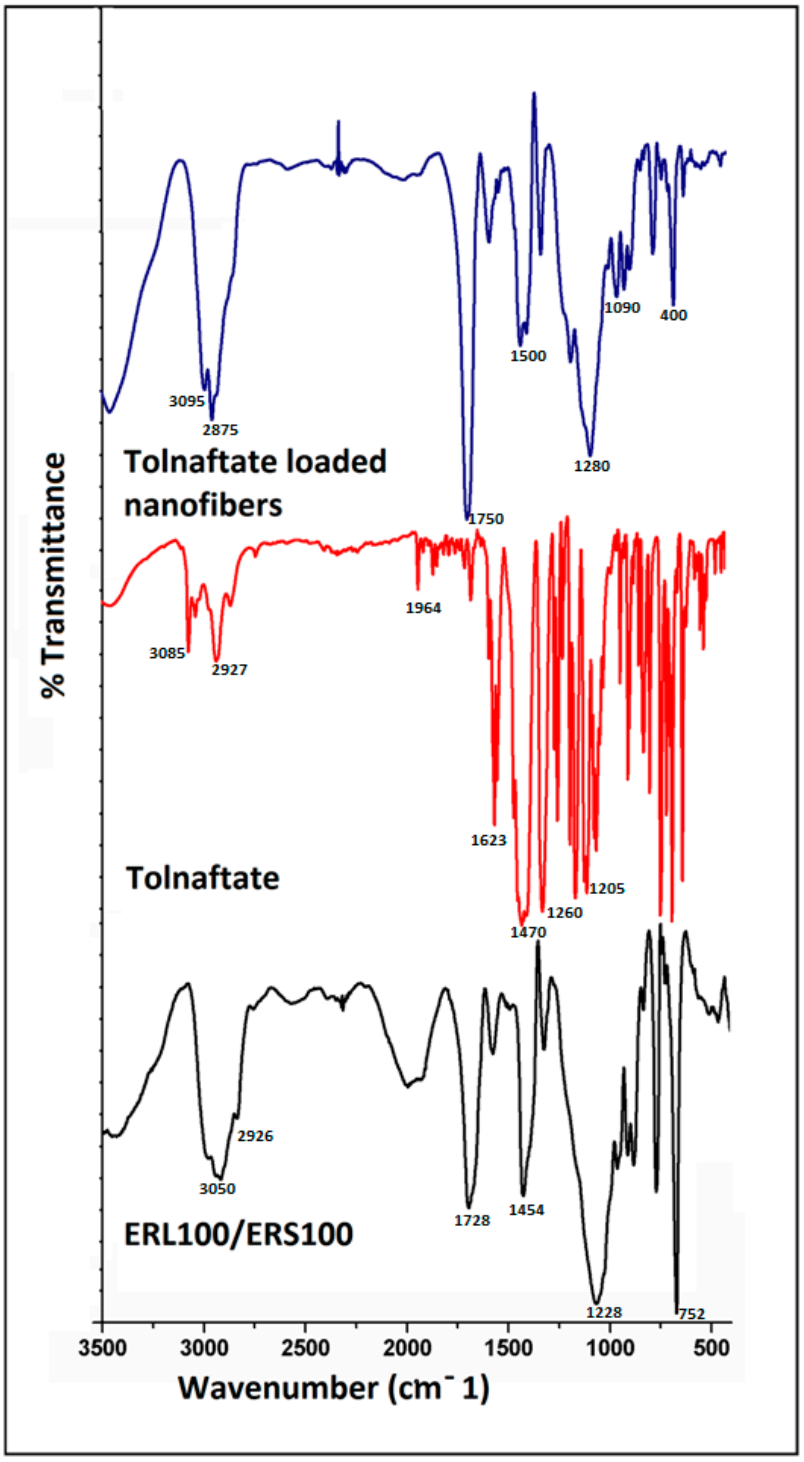


**Figure 3.** Comparative ATR-FTIR depicting specific peaks of functional groups present in the blend of ERL100/ERS100, tolnaftate, and tolnaftate-loaded nanofibers.

The TGA curve of tolnaftate demonstrated that significant weight loss at 110 °C might be the melting point of the drug. Again, at 340 °C, a degradation in weight occurred, attributed to the decomposition of its meta-disubstituted phenyl moiety. However, the TGA graph of both polymers reveals that they were decomposed at 350 °C, and fabricated nanofibers were found to be thermally stable up to 450 °C, as can be observed in Figure 4a. The X ray diffractogram of tolnaftate revealed presence of different peaks at 11°, 15°, 17°, 21°, 23°, and 26°, which better explained its crystalline state. On the contrary, the blend of ERL100/ERS100 showed a metastable crystalline nature in the diffractogram in Figure 4b. Similarly, powder X-ray portrait of tolnaftate-loaded nanofibers showed slight broad peak, which must have been due to the molecular dispersion between meta-stable polymers and crystalline tolnaftate.

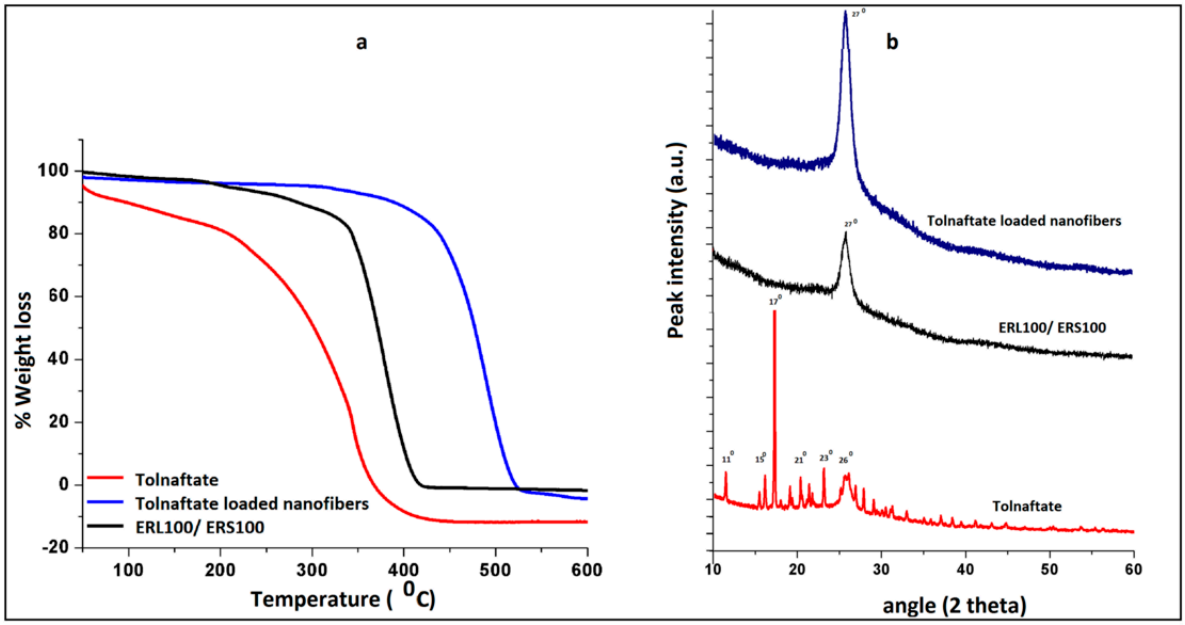


**Figure 4.** TGA portrait revealing thermal behavior of polymers ERL100/ERS100, tolnaftate, and tolnaftate-loaded nanofibers (**a**); Comparative PXRD portrait of ERL100/ERS100, tolnaftate, and tolnaftate-loaded nanofibers (**b**).

### 3.1.3. Swelling Index and In Vitro Drug Release

D3 nanofibers showed highest swelling index (Figure 5a) must be attributed to presence of higher concentration of ERL100 in it. Our previous research reported that polymer ERL100 contain high amount of quaternary ammonium compound leading higher permeability [27] across network of nanofibers in selected media. The narrow interconnected pores in D3 nanofibers must have caused a greater absorption of media and ultimately led to excellent swelling. Although the degree of swelling was found to be decreased after 8 h, the reason behind this could be degradation of integrity of polymeric nanofibers in simulated body fluid.

The presence of PEG 400 facilitated the quick hydration of nanofibers and expedited the absorption of dissolution media, which must have formed wet channels from the surrounding environment. An initial burst release was observed, which might have been due to the presence of a certain amount of drug on the surface of the fibers, which is desirable for invading and eradicating dermatophytes at the prelim stage. This was followed by a slow and controlled release of the drug lasting up to 8 h, which favored constant antifungal action in the nanofibrous scaffold. An extended drug release of 71.52% from the D3 nanofibers was due to a higher concentration of ERL100, whereas D1 nanofibers restricted the free access of the dissolution medium into the nanofiber network and released only 43.56% over an 8 h period (Figure 5b). However, D2 nanofibers showed a customized drug release

of 47.01%, attributed to the presence of an equal ratio of the two polymers. The release behavior was also supported by the swelling studies, where the degree of swelling was found to be increased after 2 h, indicating that the release mechanism is predominantly governed by the diffusion process. D3 nanofibers were pursued for further studies against the inhibition of dermatophytes.

In vitro antifungal activity through the microdilution assay showed the preeminent antifungal activity of D3 nanofibers against *T. rubrum* (95.981%). However, the rest of the dermatophytes were found to be less susceptible against D3 nanofibers, and % growth inhibition was reported as *M. canis* (78.326%), *M. fulvum* (85.789%), and *M. gypseum* (81.826%), respectively, after 96 h (Figure 6).

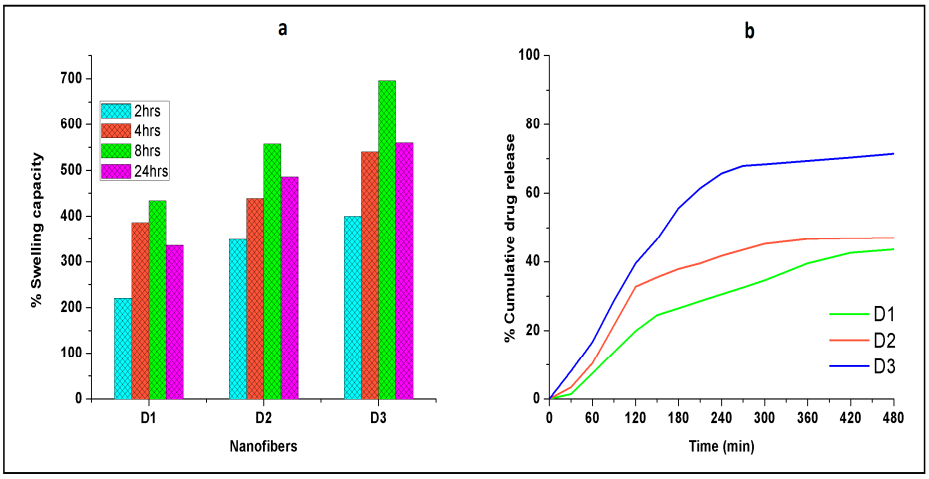


**Figure 5.** Comparative swelling index of fabricated D1, D2, and D3 nanofibers over 24 h (**a**); In vitro drug release profile of drug-loaded nanofibers in simulated phosphate buffer, pH 6.8, for 8 h (**b**).

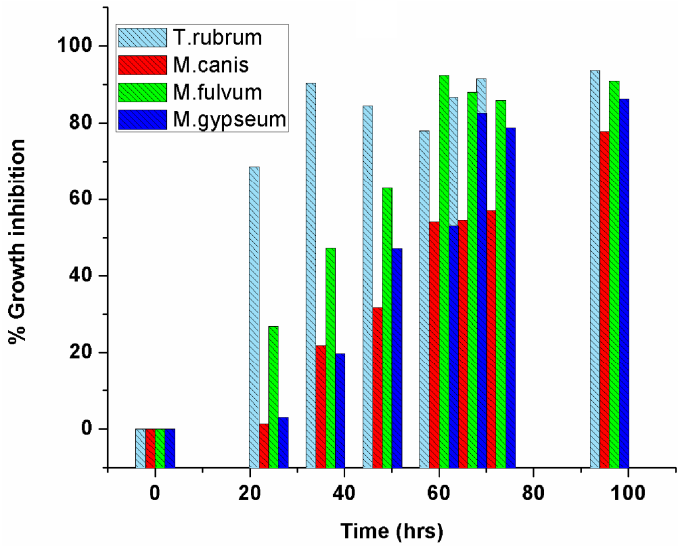


**Figure 6.** In vitro antifungal study of D3 nanofibers against *T. rubrum*, *M. canis*, *M. fulvum*, and *M. gypseum* for 96 h.

### 3.1.4. In Vivo Study

After inoculation with dermatophyte *T. rubrum*, the first symptoms, small scaly redness and erythema on the dorsal surface of mice, were observed, and these symptoms continuously increased over the study period (Figure 7a,c). The treatment was started with a topical application of the tolnaftate drug and fabricated tolnaftate-loaded D3 nanofibers for seven days. It was observed that mice treated with the pure tolnaftate had symptoms of dermatophytosis on the dorsal surface, where

supreme in vivo efficiency of D3 nanofibers was visualized. This might be due to the continuous diffusion of the tolnaftate drug from the nanofibers at a controlled rate, which functionally created a depot at the infected site with no adverse effects. The growth of hair without any scaly or patchy dorsal surface could be seen after seven days of treatment (Figure 7d). Finally, to ensure the complete eradication of the human dermal pathogen *T. rubrum* from the dorsal surface of cured mice, a small quantity of skin was scrapped from the treatment area, cultured on sabouraud dextrose agar (SDA) plates, and incubated for 14 days to check for any signs of fungal colonies. All SDA plates were vacant from growth of dermatophyte *T. rubrum*.

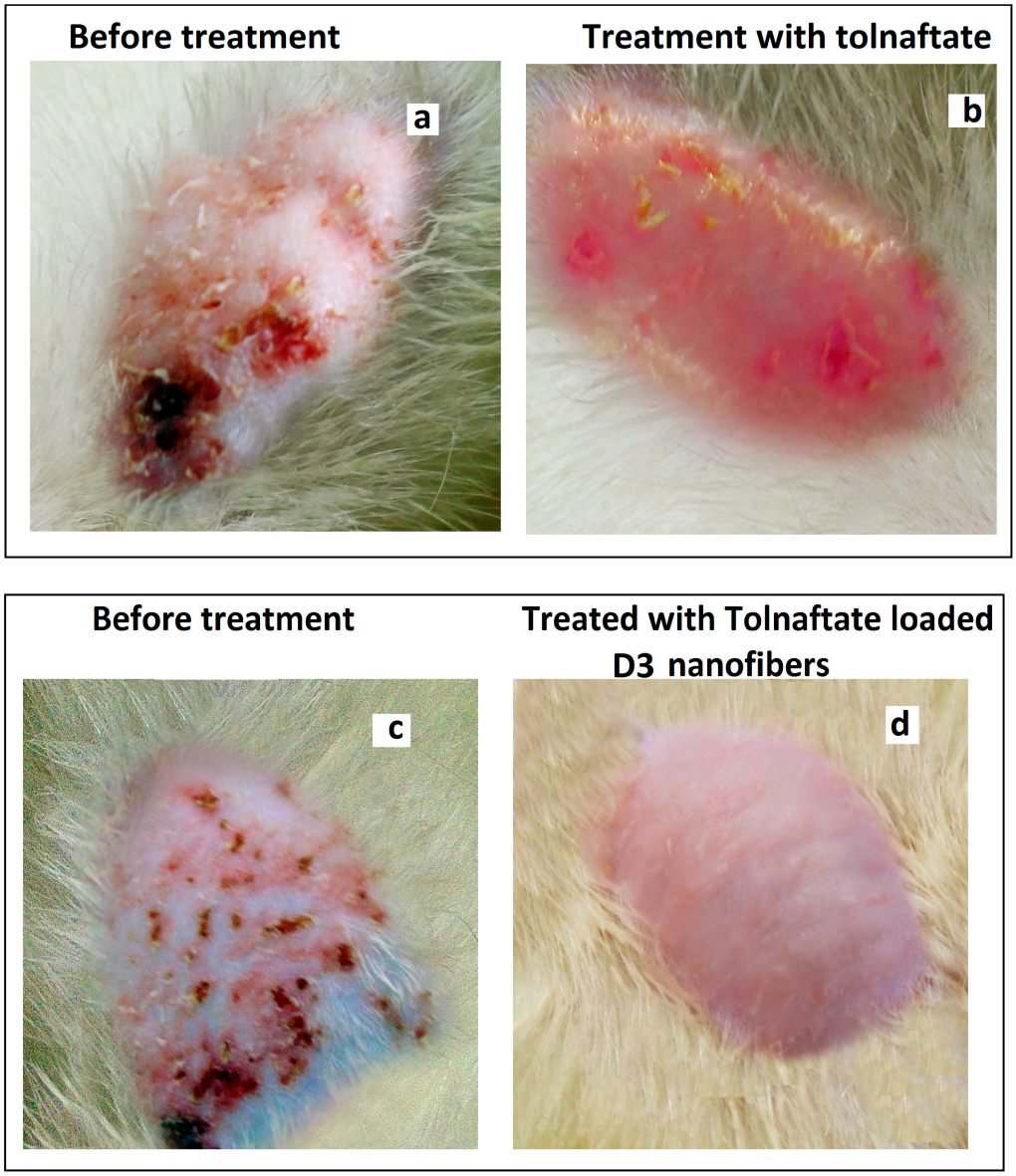


**Figure 7.** In vivo study on Swiss albino mice infected by *T. rubrum* dermatophyte (**a**,**c**); treatment with the tolnaftate drug and tolnaftate-loaded nanofibers (**b**,**d**) respectively.

## 4. Conclusions

In the present investigation, tolnaftate loaded polyacrylate polymeric nanofibers were successfully electrospun. The effect of polymeric concentration on surface morphology, fiber diameter, hydrophilicity, swelling index, and drug release were examined. All fabricated nanofibers acquired were nanoscaled with a non-beaded, defect-free, and regular appearance. The surface morphology of

the fabricated nanofibers presents an interesting perspective in terms of tailoring the multifunctional aspect of wound healing and dressing materials for topical fungal infection. The D3 nanofibers fabricated from the blend of ERL100/ERS100 (3:1) presents an excellent degree of swelling behavior that encourages the design of bioactive antifungal scaffolds with a superb capacity to absorb released exudates during dermatophytic infection. In vitro drug release studies anticipated the controlled drug release from D3 nanofibers up to 8 h. Findings from the broth dilution assay allow us to conclude significant growth inhibition of D3 nanofibers against *T. rubrum* and poor activity against *M. canis* dermatophyte. A resistant attitude of *M. canis* for tolnaftate-loaded nanofibers was clear. An animal study was conducted in *T. rubrum* infected Swiss albino mice, and a complete sign of cure was achieved after treating the mice with applied nanofibrous scaffolds successively for seven days, which acted as a depot and released tolnaftate in a controlled manner. Findings also endorsed a new purview of Eudragit polymer blends (ERL100/ERS100) for the fabrication of wound dressings (bandages/scaffolds) and biomedicine by virtue of their exclusive chemical composition. These nanofibers could contribute biocompatibility, absorb exudates, maintain moisture balance, and provide a localized effect by virtue of the depot drug at the target site, thus avoiding the reoccurrence of dermatophytosis. Further, the fabrication of nano-engineered anti-dermatophytic dressing materials/bandages embedded with a composite developed from an amalgamation of antifungal therapeutic agents and bioactive carbon allotropes will inspire new laboratory experiments and commercial applications.

**Acknowledgments:** We thankfully acknowledge the authorities and staff members of Chemical Engineering, IIT Kanpur and Botany Department, University of Allahabad, for generously granting all working facilities and extending their grudgeless cooperation.

**Conflicts of Interest:** The authors declare no conflict of interest.

## References

1. Peres, N.T.; Maranhao, F.C.; Rossi, A.; Martinez-Rossi, N.M. Dermatophytes: Host pathogen interaction and antifungal resistance. *An. Bras. Dermatol.* **2010**, *85*, 657–667. [CrossRef] [PubMed]
2. Elmegeed, A.S.M.A.; Ouf, S.A.; Moussa, T.A.A.; Eltahlawi, S.M.R. Dermatophytes and other associated fungi in patients attending to some hospitals in Egypt. *Braz. J. Microbiol.* **2015**, *46*, 799–805. [CrossRef] [PubMed]
3. Prescott, M.L.; Harley, J.P.; Donald, A.K. *Microbiology*, 5th ed.; McGraw Hill Publishers: New York, NY, USA, 2003.
4. Nosanchuk, J.D. Current status and future of antifungal therapy for systemic mycoses. *Recent Pat. Anti-Infect Drug Discov.* **2006**, *1*, 75–84. [CrossRef]
5. Yamaguchi, H.; Uchida, K.; Tanaka, T.; Yamaguchi, T. Therapeutic efficacy of a topical tolnaftate preparation in guinea pig model of tinea pedis. *Jpn. J. Antibiot.* **2001**, *54*, 323–330. [PubMed]
6. Weinstein, M.J.; Oden, E.M. Antifungal properties of tolnaftate in vitro and in vivo. *Antimicrob. Agents Chemother.* **1964**, *10*, 595–601. [PubMed]
7. Kuzetyte, T.; Drevinskas, T. Study of tolnaftate release from fatty acids containing ointment and penetration into human skin ex vivo. *Acta Pol. Pharm.* **2011**, *68*, 965–973.
8. Sun, K.; Li, Z.H. Preparations, properties and applications of chitosan based nanofibres fabricated by electrospinning. *eXPRESS Polym. Lett.* **2011**, *5*, 342–361. [CrossRef]
9. Camposeo, A.; Greenfeld, I.; Tantussi, F.; Moffa, M.; Fuso, F.; Allegrini, M.; Zussman, E.; Pisignano, D. Local mechanical properties of electrospun fibres correlate to their internal nanostructure. *Nano Lett.* **2013**, *13*, 5056–5062. [CrossRef] [PubMed]
10. Jaishri Sharma, J.; Lizu, M.; Stewart, M.; Zygula, K.; Lu, Y.; Chauhan, R.; Yan, X.; Guo, Z.; Wujcik, E.K.; Wei, S. Multifunctional nanofibers towards active biomedical therapeutics. *Polymers* **2015**, *7*, 186–219. [CrossRef]
11. Khil, M.S.; Cha, D.I.; Kim, I.; Bhattarai, N. Electrospunnano fibrous polyurethane membrane as wound dressing. *J. Biomed. Mater. Res.* **2003**, *67*, 675–679. [CrossRef] [PubMed]
12. Rho, K.S.; Jeong, L.; Lee, G.; Seo, B.M.; Park, Y.J.; Hong, S.D.; Roh, S.; Cho, J.J.; Park, W.H.; Min, B.M. Electrospinning of collagen nanofibres: Effects on the behavior of normal human keratinocytes and early stage wound healing. *Biomaterials* **2006**, *27*, 1452–1461. [CrossRef] [PubMed]

13. Rieger, K.A.; Birch, N.P.; Schiffman, J.D. Designing electrospun nanofiber mats to promote wound healing—A review. *J. Mater. Res.* **2013**, *67*, 675–679. [CrossRef]
14. Pendekal, S.M.; Tegginamate, P.K. Formulation and evaluation of a bioadhesive patch for buccal delivery of tizanidine. *Acta Pharm. Sin. B* **2012**, *2*, 318–324. [CrossRef]
15. Bucolo, C.; Maltese, A.; Puglisi, G.; Pignatello, R. Enhanced ocular anti-inflammatory activity of ibuprofen carried by an Eudragit RS 100 nanoparticle suspension. *Ophthalmic Res.* **2002**, *34*, 319–323. [CrossRef] [PubMed]
16. Ravelli, D.; Merli, D.; Quartarone, E.; Profumo, A.; Mustarelli, P.; Fagnoni, M. PEGylated carbon nanotubes: Preparation, properties and applications. *RSC Adv.* **2013**, *3*, 13569–13582. [CrossRef]
17. Garg, K.; Bowlin, G.L. Electrospinning jets and nanofibrous structures. *Biomicrofluidics* **2011**, *5*, 013403. [CrossRef] [PubMed]
18. Zargham, S.; Bazgir, S.; Tavakoli, A.; Rashidi, A.S.; Damerchely, R. The Effect of Flow Rate on Morphology and Deposition Area of Electrospun Nylon 6 Nanofiber. *J. Eng. Fiber Fabr.* **2012**, *7*, 42–49.
19. Reneker, D.H.; Yarin, A.L. Electrospinning jets and polymer nanofibers. *Polymer* **2008**, *49*, 2387–2425. [CrossRef]
20. Huang, F.L.; Wang, Q.Q.; Wei, Q.F.; Gao, W.D.; Shou, H.Y.; Jiang, S.D. Dynamic wettability and contact angles of poly (vinylidene fluoride) nanofiber membranes grafted with acrylic acid. *eXPRESS Polym. Lett.* **2010**, *4*, 551–558. [CrossRef]
21. Siddiqui, A.R.; Maurya, R.; Balani, K. Superhydrophobic self-floating carbon nanofiber coating for efficient gravity-directed oil/water separation. *J. Mater. Chem. A* **2017**, *5*, 2936–2946. [CrossRef]
22. Choi, J.; Lee, K.M.; Wycisk, R.; Pintauro, P.N.; Mather, P.T. Nanofiber composite membranes with low equivalent weight perfluorosulfonic acid polymers. *J. Mater. Chem.* **2010**, *20*, 6282–6290. [CrossRef]
23. Pakshir, K.; Bahaedinie, L.; Rezaei, Z.; Sodaifi, M.; Zomorodian, K. In Vitro activity of six antifungal drugs against clinically important dermatophytes Jundishapur. *J. Microbiol.* **2009**, *2*, 158–163.
24. Padhan, D.K.; Pattnaik, S. In vivo antifungal activity of Accmella essential oil on a dermatomycotic strain Trichophyton mentagrophytes (MTCC-7687). *Pharm. Sin.* **2014**, *5*, 40–44.
25. Ameri, A.; Rajive, B.; Vaidya, J.G.; Apte, K.; Deokule, S.S. Anti-Staphylococcal and wound healing activities of Ganoderma praelongum and Glycyrrhiza glabra formulation in mice. *Int. J. Appl. Res. Nat. Prod.* **2013**, *6*, 27–31.
26. Tiaan, D.J.; Smith, H.C.; Dicks, L.M.T. Evaluation of a Nisin-Eluting Nanofiber Scaffold to treat Staphylococcus aureus-Induced Skin Infections in Mice. *Antimicrob. Agents Chemother.* **2013**, *57*, 3928–3935.
27. Pandey, H.; Sharma, U.K.; Pandey, A.C. Eudragit based nanostructures: A potential approach for ocular drug delivery. *Int. J. Res. Dev. Pharm. Life Sci.* **2012**, *1*, 40–43.